Estimation of systematic errors in the GFS using Analysis Increments

Kriti Bhargava[1], Eugenia Kalnay[1], James A. Carton[1], and Fanglin Yang[2]

[1]Department of Atmospheric and Oceanic Science, University of Maryland, College Park, MD 20742

[2]NOAA/National Weather Service National Centers for Environmental Prediction, 5830 University Research Court, College Park, MD 20740

Corresponding author: Kriti Bhargava (kritib@umd.edu)

Key Points:

- Global Forecast System model has robust, systematic seasonal mean and diurnal forecast errors due to biases of the model and observations
- 6-hr analysis increments estimate the model bias before the errors grow nonlinearly, and can be used to correct the model "online".
- Observation and model bias corrections within the Analysis Increments can be separated by their impact on systematic forecast errors.

Abstract

We estimate the model deficiencies in the Global Forecasting System (GFS) that lead to systematic forecast errors, as a first step toward correcting them online (i.e., within the model) as in *Danforth and Kalnay* 2008 (*DK*08). Since the Analysis Increments represent the corrections that new observations make on the 6-hr forecast in the analysis cycle, we estimate the model bias corrections from the time average of the analysis increments divided by 6-hr, assuming that initial model errors grow linearly and first ignoring the impact of observation bias. During 2012-2016, seasonal means of the 6-hr model bias are generally robust despite changes in model resolution and data assimilation systems, and their broad continental scales explain their insensitivity to model resolution. The daily bias dominates the sub-monthly analysis increments and consists primarily of diurnal and semidiurnal components, also requiring a low dimensional correction. Analysis increments in 2015 and 2016 are reduced over oceans, which we attribute to improvements in the specification of the SSTs. These results provide support for future efforts to make online correction of the mean, seasonal and diurnal and semidiurnal model biases of GFS to reduce both systematic and random errors, as suggested by *DK*08. It also raises the possibility that analysis increments can also provide guidance in testing new physical parameterizations.

1 Introduction

The performance of numerical weather prediction models is limited by errors in the model forecasts resulting from the errors in initial conditions and model deficiencies. Model forecast errors can be classified into random errors, whose time average is zero, and systematic errors [*Dalcher and Kalnay*, 1987, *Murphy*, 1988]. We define forecast error as the difference between a model forecast x_f and a verifying analysis assumed to represent the truth x_t, and separate the mean square error into the systematic and random components:

$$\overline{(x_f - x_t)^2} = (\overline{x_f} - \overline{x_t})^2 + \overline{(x_f' - x_t')^2} \quad (1)$$

where the overbars represent a time average (such as a month or a season), and the primes represent the departures from this average. We will refer to the square root of the first term of the rhs (i.e., the time mean of the error) as the systematic forecast error, and the square root of the second term (error variance) as the non-systematic or random errors.

Systematic forecast errors (SFEs) are a significant portion of the total forecast error in weather prediction models, such as the Global Forecast System (GFS). Fig. 1 shows that after two weeks, the range of GFS RMS temperature systematic errors reach 1/3 of total temperature forecast error. Many studies attribute SFEs to specific deficiencies in numerical discretization of the equations of motion, parameterizations of sub-grid processes, or boundary conditions (e.g., *Jung and Tompkins*, 2003; *Zheng et al.*, 2006, 2009) which lead to model bias. These errors are initially small, but as the model is integrated in time the errors grow and interact nonlinearly with systematic and random errors until the model loses all forecast skill. The SFEs include mean and periodic forecast bias, the latter including those associated with the annual cycle and the diurnal cycle, and also state-dependent errors associated with the presence of short- or long-term anomalies, such as weather highs and lows, or the phase of El Niño [*Danforth et al*., 2007]. In this paper, we aim to estimate the GFS model bias that leads to SFEs in the period 2012-2016. In addition to suggesting causes for these model errors and exploring the impact of changes in the GFS system, we evaluate their potential use as input to an empirical online correction scheme as introduced by *Danforth and Kalnay* [2008].

The GFS is a global numerical weather prediction model which provides 16-day forecasts produced by the National Centers for Environmental Prediction (NCEP). It couples an atmosphere model, a sea-ice model and a land/soil model using specified sea surface temperatures (SSTs) as boundary conditions to produce the forecasts. It is initialized with the Global Data Assimilation System (GDAS). Details about GFS are discussed in section 2.

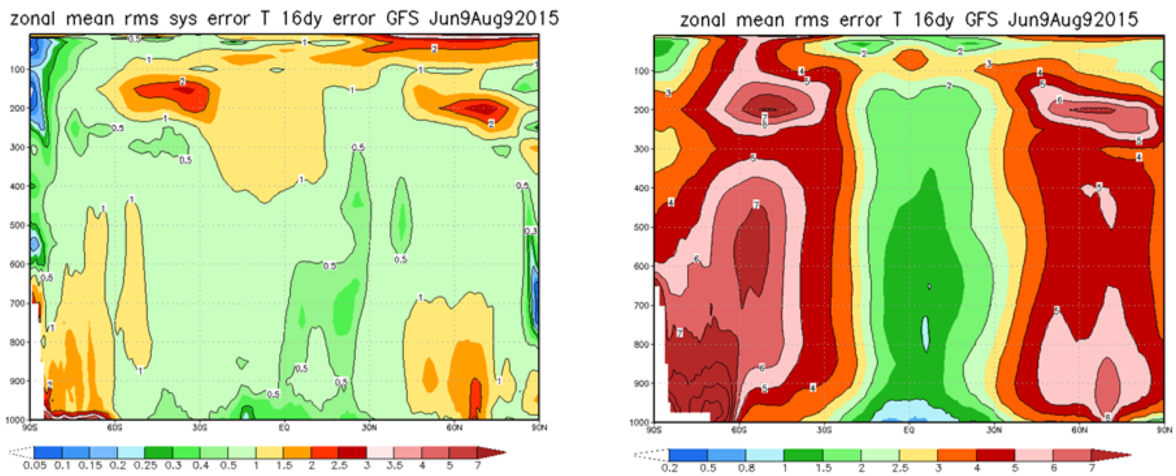

Figure 1. Zonal mean RMS systematic error (left) and total error (right) in temperature after 16 days. The range of temperature systematic errors is ~1/3 of total temperature error range after 2 weeks. (Courtesy of Dr. Glenn White).

The earliest attempts to estimate model bias within the predecessors to GFS for the purpose of correcting them online, were made by Saha and colleagues [*Johansson and Saha*, 1989; *Saha* 1992]. They calculated the bias by averaging the error in 1-day forecasts over a training period of fixed length. After testing training periods ranging from 5 to 70 days, they found that the training period between 25-30 days improved the 5-day forecast while longer training periods improved longer forecast times. Though mostly successful, the biases were not always reduced using this method. The authors concluded that their systematic model bias estimation method contained large sampling errors and suggested other ways to estimate biases.

Among the more recent studies proposing to estimate and correct model bias, *Danforth et al.* [2007] (*DKM*07 hereafter) used the low resolution SPEEDY general circulation model and initialized it from the NCEP-NCAR Reanalysis [*Kalnay et al.*, 1996]. *DKM*07 computed the model bias as the difference between six-hour forecasts variables and the corresponding analysis variables, averaged over many forecasts. They separated the 6-hr systematic model errors into time averaged model bias, periodic bias and state dependent error. They pointed out that the forecast system could be corrected for the time average bias by adding the average bias correction term divided by 6-hr to the time derivative of each model variable.

$$\dot{x}(t) = M[x(t)] + \frac{\overline{\delta x_6^{ai}}}{6-hr} \qquad (2)$$

Here, M[x(t)] is the standard model tendency to which the correction is added.

Various empirical forecast error correction schemes have been used to correct the forecasts based on the analysis of mean and variance of past model forecast errors. The simplest correction schemes operate "offline" (after the forecast is completed), applying a different statistical correction for each forecast length. A disadvantage of the offline correction schemes is that they allow forecast errors to grow until the end of the forecast cycle before comparing them with the verifying analyses and making an average correction. During the 2- week period in which errors grow until they saturate, the errors interact nonlinearly, obscuring their origin. The other type of correction scheme, used by *Saha* [1989], *DKM*07, *DelSole et al.* [2008], and others, is "online" (applied during the model integration) as in equation (2). This scheme attempts to estimate and correct the bias during the model integration.

Danforth and Kalnay [2008, *DK*08 hereafter] showed that the online correction of the model bias estimated by *DKM*07 not only worked as well as the offline statistical correction of the systematic errors, but that it also reduced the random errors, indicating that the correction of the model bias actually did improve the model. *DKM*07 could further reduce systematic errors significantly by correcting for diurnal cycle errors.

DelSole et al. [2008] used the Center for Ocean-Land-Atmosphere (COLA) land-atmosphere model (v3.2) to test different methods to reduce the systematic errors. They estimated the 24-hr model bias using an autoregressive model with a decorrelation time of 2 days, and found that the online correction method was able to reduce the systematic errors but could not reduce random errors by correcting for model bias. By contrast, *DK*08 estimated and corrected online the model bias directly from the time averaged bias of the 6-hr forecast. *DelSole et al.* [2009] suggested a possible alternative approach similar to the one used by *DKM*07 and *DK*08, but did not use it. *DelSole et al.* [2008, 2009] concluded that it was impossible in a realistic model/data assimilation system to estimate the model bias and correct it, and thus reduce not only systematic errors but random errors as well.

In this paper, we apply a methodology similar to *DKM*07 to the NCEP operational GFS/GDAS system, estimating the mean and periodic model biases from the 6-hr analysis increments (AIs), before the forecast errors grow non-linearly. AIs are the difference between the gridded analysis and forecast, with the former providing our best gridded estimate of the true state of the atmosphere. In Section 2, we estimate the 6-hr GFS model bias from the average 6-hr operational GDAS AIs. In Section 3, we examine the structure and evolution of the biases, and compare the bias correction for the 2012-2014 period, during which few model changes took place, to the final 2015-2016 period where major model and changes to the SST boundary condition took place. In section 4, sub-monthly periodic biases are estimated and represented using EOFs to provide evidence that a low dimensional approach can also be used to correct the dominant diurnal and semi-diurnal errors. A summary and discussion of the results and details regarding the online correction experiments that we plan to perform with the estimated systematic and daily errors is presented in section 5.

2 Materials and Methods

The GFS is a three-dimensional hydrostatic global spectral model with current operational resolution of T1534 from 0-10 days and T574 from 10-16 days. The model uses 64 hybrid sigma levels [*Sela*, 2009] in the vertical, defined as: p(x,y,t) = $\sigma_1 p_s + \sigma_2$ so that they become parallel pressure levels at high altitudes, σ_1 and σ_2 are parameters, and p_s is sea level pressure. Here we present results at 7 representative model levels, including the bottom two levels, the top level, and five model levels in between (Table 1). The GFS is run four times a day and forecasts are issued every hour for the first 12 hours, then every 3 hours for up to 10 days and then every 12 hours. The GFS analysis is run twice per cycle: the "early" GFS run that provides 16-day forecasts, and the "final" GDAS (Global Data Assimilation System) run that assimilates late-arriving observations and provides a "final" analysis for the GFS. The GDAS currently uses a hybrid four-dimensional ensemble variational formulation [*Buehner et al.*, 2013].

Table 1. Model levels shown and their parameters

Model Level	Parameter (σ1)	Parameter (σ2)	Pressure if Ps =1000 mb
1	1	0	1000
2	0.995	0	995
7	0.954	116.899	950
14	0.827	2051.15	850
25	0.393	12344.49	500
35	0.506	15683.489	200
64	0	64.27	0

The GFS/GDAS system is updated regularly to improve its performance. At the beginning of our study period, January 2012, the GDAS was based on the 3D-VAR Global Spectral Interpolation [*Wu et al*., 2002]. It used T574 resolution semi-implicit Eulerian discretization, with the lower SST boundary condition over the oceans provided by the weekly averaged Optimal Interpolation SST [*Reynolds and Smith*, 1994]. Beginning in May 2012, a hybrid 3DVar-ENKF data assimilation system [*Wang et al.,* 2013], which makes use of a background error estimate from a combination of a lower resolution Ensemble Kalman Filter and a static background error, replaced the prior gridpoint statistical interpolation. In January 2015, GFS transitioned to a two time-level T1534 semi-implicit semi-Lagrangian discretization, and switched to the high resolution daily real time global SST product [*Thiébaux et al*., 2003]. In May 2016, the hybrid data assimilation system was upgraded to the current operational 4D hybrid ensemble-variational data assimilation system [*Buehner et al*., 2013]. Assimilation of new radiances from Advanced Microwave Sounding Unit was also added. The details of the evolution of GFS are described at: www.emc.ncep.noaa.gov/gmb/STATS/html/model_changes.html.

To estimate the model bias, we take advantage of the GDAS, which optimally combines the 6-hr forecast, or background, with the new observations, creating a new analysis. The analysis is the best estimate of truth we have after combining the model forecasts and the observations. The AIs are thus the estimated correction that the new observations make upon the 6-hr forecast. Therefore, we can use the time average of the AIs as the model bias correction over 6 hr, the negative of which is the 6-hr model bias. An important advantage of this approach is that over 6-hr, the forecast error growth is linear [*Klinker and Sardeshmukh*, 1992, *Vannitsem and Toth*, 2002; *Jung and Tompkins*, 2003; *Xue et al*. 2013 and 2015]. Hence, the average 6-hr AIs give the best estimate of the model bias before the errors start growing non-linearly.

We use the 6-hr analysis and forecasts for surface pressure, temperature, winds and specific humidity provided by the operational GFS. The GFS horizontal resolution was T574 until January 2015 when it transitioned to T1534. For convenience, we remap variables through the full period of interest 2012-2016 onto a uniform lower resolution T254 grid, to match the resolution at which we have access to the AIs. This reduction in resolution has essentially no impact on our analysis, as illustrated in Fig. 2. We begin by focusing on seasonal model bias correction, which we estimate as the seasonal average (DJF, MAM, JJA, and SON) of the AIs during the five years 2012-2016. The temporal stability of the seasonal bias is evaluated, by comparing the spatial patterns of the seasonal AIs for the first three years (2012-2014) and evaluating their similarity using anomaly correlations.

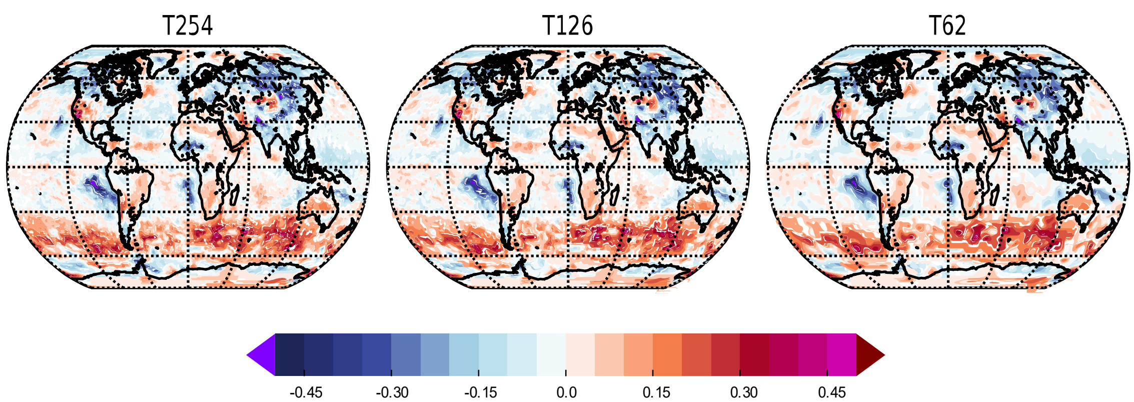

Figure 2. 6-hour model bias for July 2014 surface temperature projected on three spatial resolutions: T254, the original resolution of data provided, (left), T126 (middle) and T62 (right). The patterns of bias remain essentially the same, indicating that the scales of the model bias are well resolved by T62.

To identify the systematic components of the periodic AIs at sub-monthly scales we first calculate the anomalies of the 6-hourly AIs with respect to their monthly averages. We then decompose these anomalies into a complete set of 120 Empirical Orthogonal Functions (EOFs) and corresponding principal component time series. These EOFs are geographically weighted, so both the spatial patterns and the time series are orthogonal over the surface of the globe. We find that these are dominated by the diurnal and semidiurnal components (see section 4).

3 Seasonal Bias

In this section, we examine the structure and evolution of the seasonal cycle biases. We begin by examining the seasonal biases and compare the bias corrections for the initial three-year period 2012-2014, during which few model changes took place, to the final 2-year period, 2015-2016 with major model and boundary condition changes.

We first explore how the global mean error in GFS forecasts changes with height. The estimated GFS error of temperature and winds is approximately 0.1K and 0.2 m/s, from the surface to level 54 (approximately 13 mb), and then becomes very large, presumably because of the effects of the artificial rigid upper boundary which introduces errors in the radiative balance and generates spurious dynamic instabilities [*Kalnay and Toth*, 1996; *Hartmann et al.*, 1996] that remain attached to the top. Specific humidity error increases from near surface to 0.1 g/kg at 850 mb, decreasing so that by 300 mb the air is dry. Here, we present results only for the surface and 850 mb.

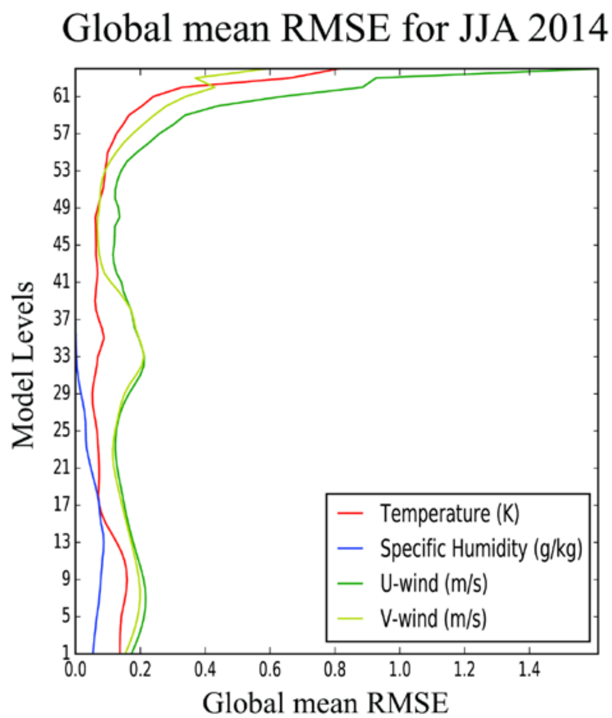

Figure 3. Global mean temperature, specific humidity and winds error vs model level for JJA 2014. The increase in error for levels above 53 is discussed in the text.

Despite major changes made to the data assimilation scheme in May 2012, the bias corrections retain their major features throughout 2012 to 2014 **(**Figs. 4 and 5**).** In general, the model tends to underestimate surface pressure over the land and overestimate it over the ocean, except the regions of warm pools at the Gulf of Mexico, North Atlantic, and Bay of Bengal **(**Fig. 4). The surface pressure bias over the land peaks in local summer and is lowest during local winter. Conversely, over ocean the high bias peaks during the local winter.

South and East Asia show a -10 to -20 mb erroneously low forecast surface pressure during JJA (Fig. 4). This is the result of erroneously warm and dry forecast air, which peaks during the summer monsoon (Fig. 5). A possible explanation is that the monsoon winds carrying moisture in from the Southern Hemisphere are erroneously weak. Near the Equator the elevated humidity associated with the ITCZ is spread too wide meridionally, with too weak convergence, so that the ITCZ itself is too dry and the Equator is too moist (Fig. 5).

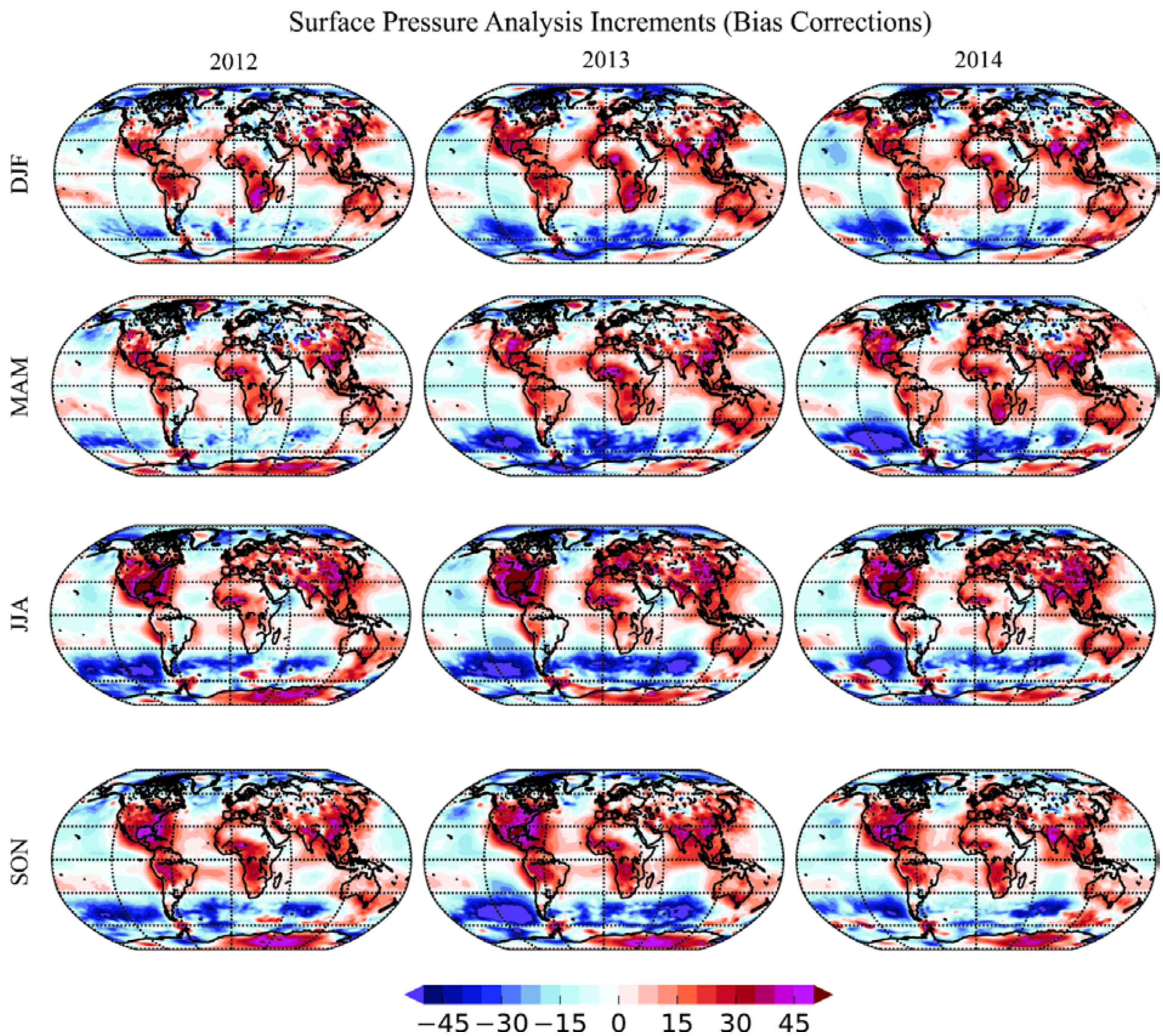

Figure 4. Seasonally averaged surface pressure AIs (mb) for 2012 to 2014 (left to right). Forecast surface pressure is generally too high (cool colors) over the oceans, except near coasts, and too low (warm colors) over the continents. Seasonal mean AIs remain relatively consistent for the 3 years.

Erroneously warm temperatures are also present over the subsidence zones west of South Africa and South America (Fig. 5). For many GCMS high temperatures in these locations are likely due to an inability to maintain sufficient stratus clouds [*Zheng et al.*, 2011; *Lien et al.*, 2016b). What is a little different here is that the biases are more strongly concentrated in the Southern Hemisphere and are displaced a few degrees westward from the coast. These areas also have a dry bias of 0.3 to 0.6 g/kg.

A cold bias is present over the oceans in higher latitudes during local summer with the bias being more prominent over the Southern Ocean. Accompanying the cold bias over the Southern Ocean is a positive surface pressure bias. Interestingly, the biases in surface pressure seemed to increase after the data assimilation changes made in May 2012. The winds in this region show a north-easterly bias. This bias pattern over the ocean in the Northern Hemisphere is also found in various GCM simulations and is hypothesized to be due to inaccuracies in simulation of North Atlantic storms [*Chapman and Walsh*, 2007]. Over the Southern Ocean (60°S-40°S) surface temperature forecasts are -0.2K/6-hr erroneously cool (Fig. 5), while the intense easterlies that dominate in this latitude zone are displaced 5° too far northward.

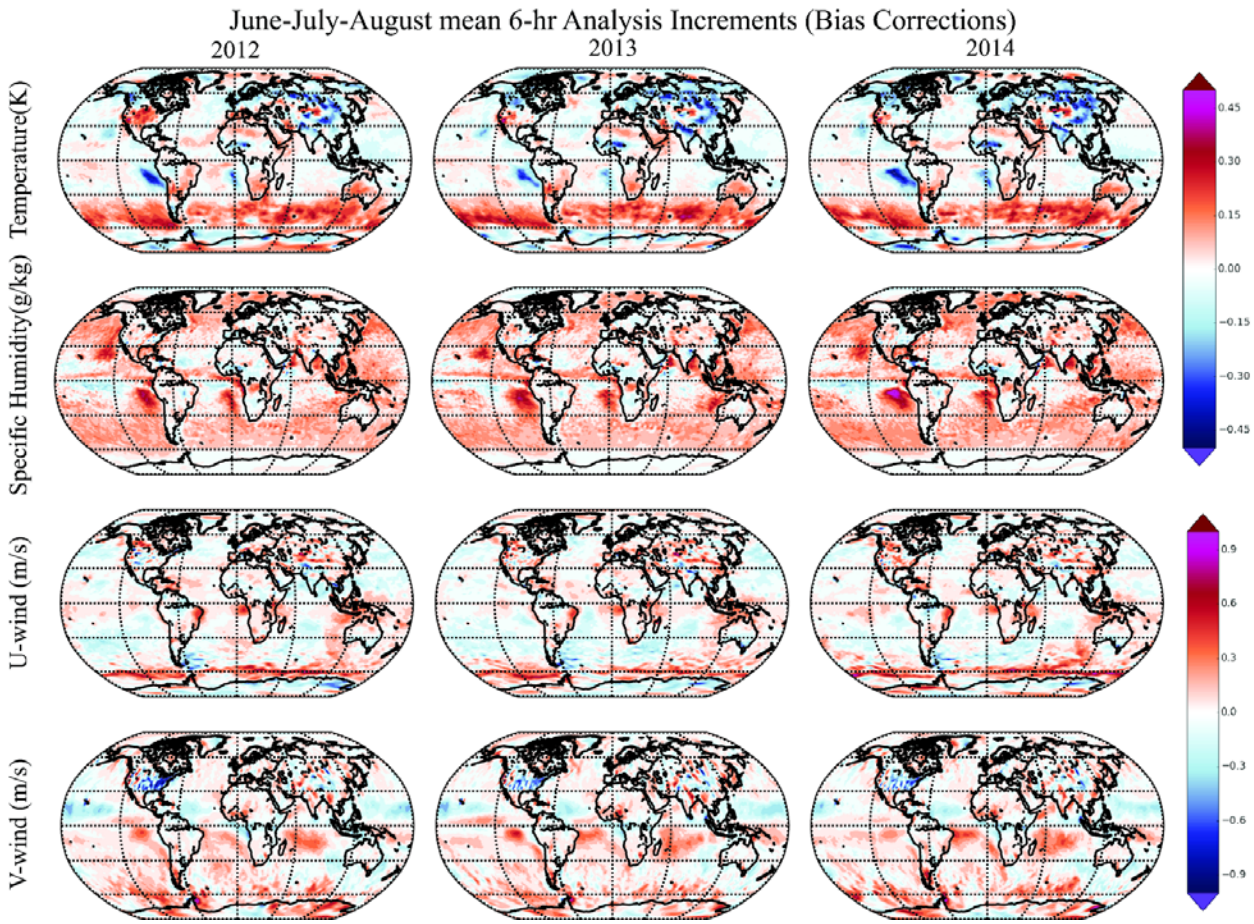

Figure 5. JJA averaged AIs for the years 2012 (left), 2013 (middle) and 2014 (right) at approximately 850 mb. The AIs remain quite consistent from 2012 to 2014.

We next explore how the AIs change when progressing from the years 2012-2014 to 2015-2016 (Fig. 6). The most striking changes occur over the oceans. There we see a reduction of the cold temperature bias, a reduction of the dry bias, and a southward shift of the Polar Front in the Southern Ocean. Model changes possibly responsible for this improvement between these periods are the shift of SSTs from the use of weekly optimally interpolated (OI) SST to the high resolution real time global (RTG) SSTs and the update of the Community Radiative Transfer Model (CRTM).

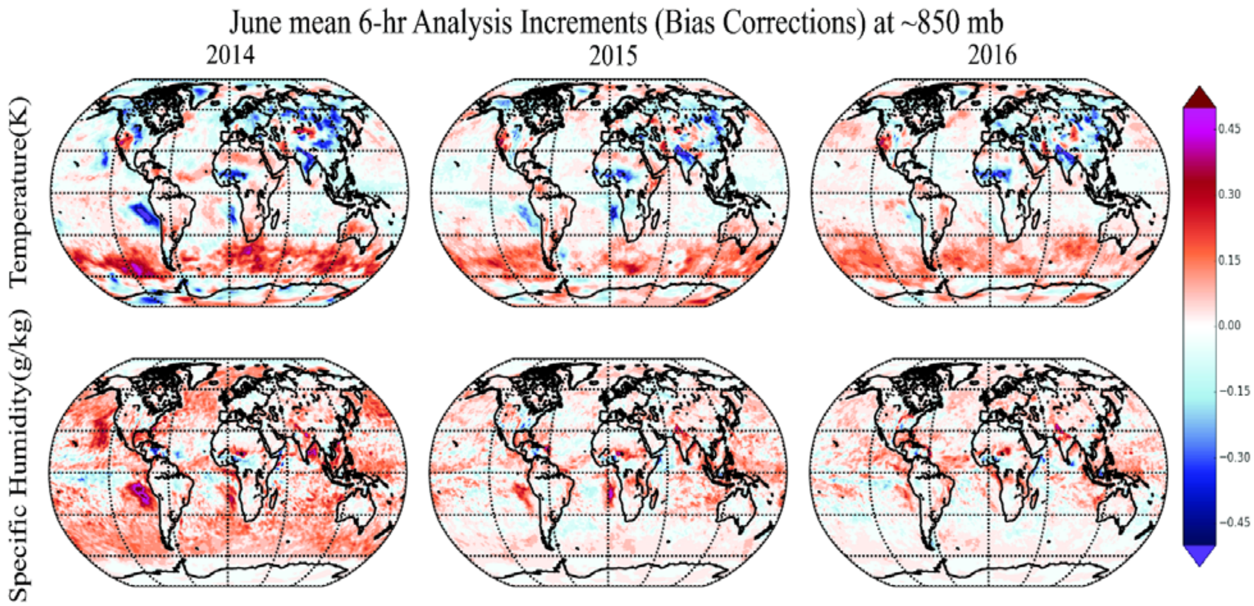

Figure 6. Temperature and specific humidity AIs for June 2014, 2015 and 2016. The errors are substantially reduced from 2014 to 2015 especially over the ocean, and further reduce in 2016.

We compared the difference between RTG and OI SSTs with the changes in AI in 2014 and 2015. In the Northern Hemisphere the surface temperature AI improvements are highly correlated with the places of significant difference between RTG and OI SSTs (Fig. 7). The warmer RTG SSTs in the north Pacific and Atlantic tend to remove the cold bias in 2015, which was found in 2012-2014. Further experiments are required to confirm the role of SST in the improvements in bias.

In contrast to the situation in the Northern Hemisphere, RTG SSTs are colder in the Southern Ocean. But we still find a reduction of cold bias in forecasted temperature. This is a result of updating the CRTM which improved the analysis of near surface temperature over water, especially in the Southern Oceans by improving specification of microwave sea surface emissivities (http://www.nws.noaa.gov/om/notification/tin14-46gfs_cca.htm,D. Kleist, pers. comm., 2017).

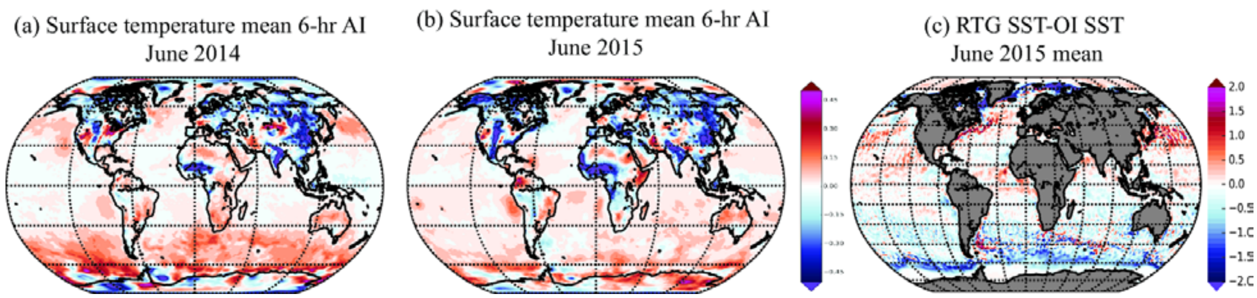

Figure 7. Comparison of change in surface air temperature mean bias, June 2014 (a) - June 2015(b) with the difference in RTG and OI SST (c). Warm colors indicate that RTG SSTs are warmer than the OI SSTs.

4 Periodic Bias Estimation

The periodic bias at sub-monthly periods is dominated by the daily cycle, which includes stationary components, a large diurnal component that progresses westward following the motion of the Sun and a significant semi-diurnal signal (Fig. 8). The size of these are comparable to the seasonal bias, thus making correction of diurnal and semi-diurnal bias also critical to improving the model performance. To separate these components, we conduct a standard EOF analysis of the 6-hourly AIs each month and then focus on those terms associated with the daily cycle.

Over the eastern Atlantic and Pacific Oceans, the model tends to overestimate humidity and underestimate temperature during daytime and underestimate night-time humidity and overestimate night-time temperature. The bias has a semi-diurnal component during the southwest monsoon season JJA over Europe and Asia, with peaks in cold bias both in early morning and dusk and warm bias late morning and night.

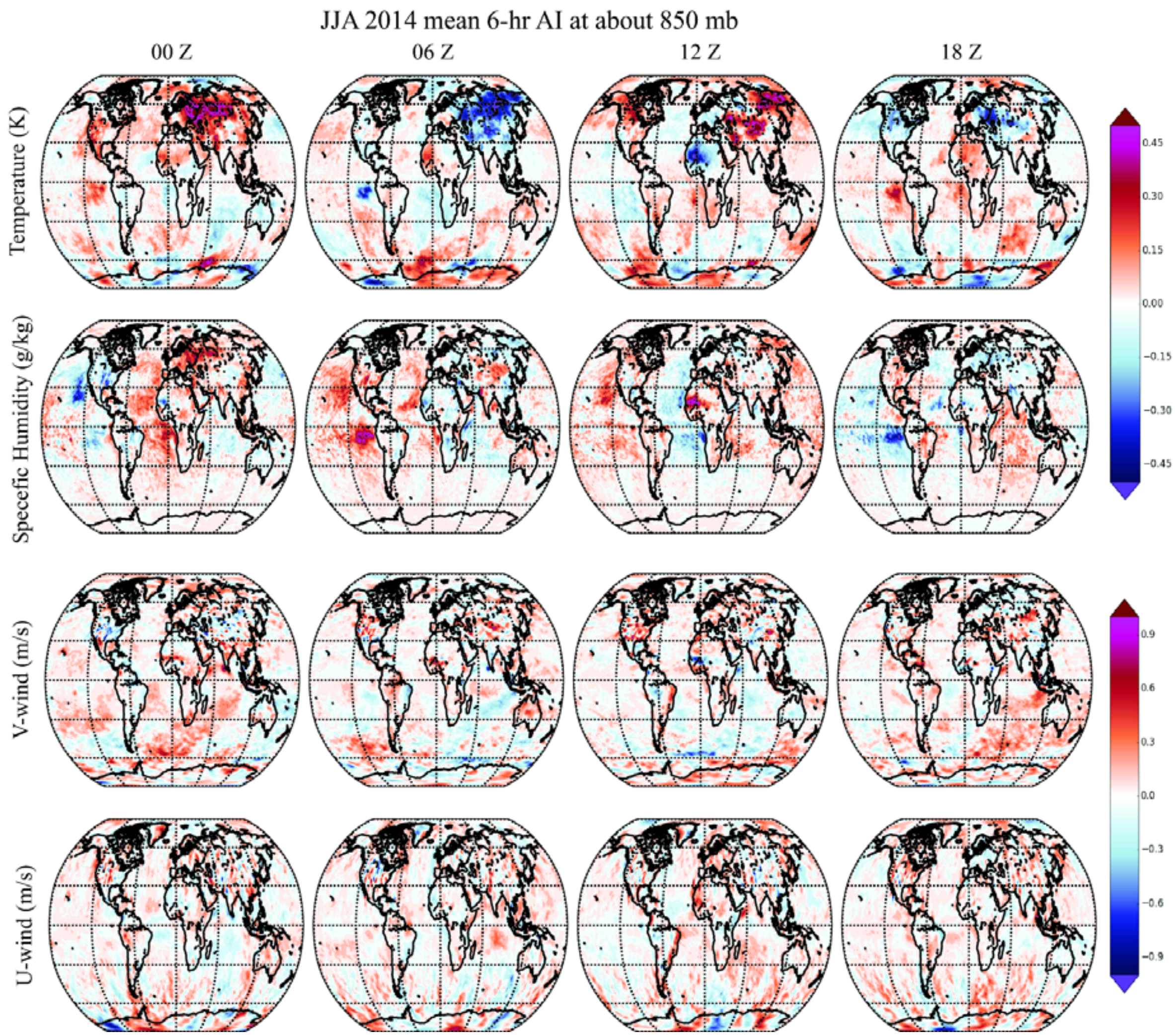

Figure 8. JJA AIs for 2014, at 00 Z to 18 Z (from left to right) for temperature, specific humidity, zonal and meridional winds (top to bottom) at approximately 850 mb.

The monthly EOFs, which consist of 120 modes, are dominated by the four leading daily modes which explain 24% (surface pressure), 11% (temperature), and 10% (humidity), and nearly completely describe the daily cycle (Fig. 9). The diurnal cycle biases in 2015 and 2016 show similar structure with reduced magnitude.

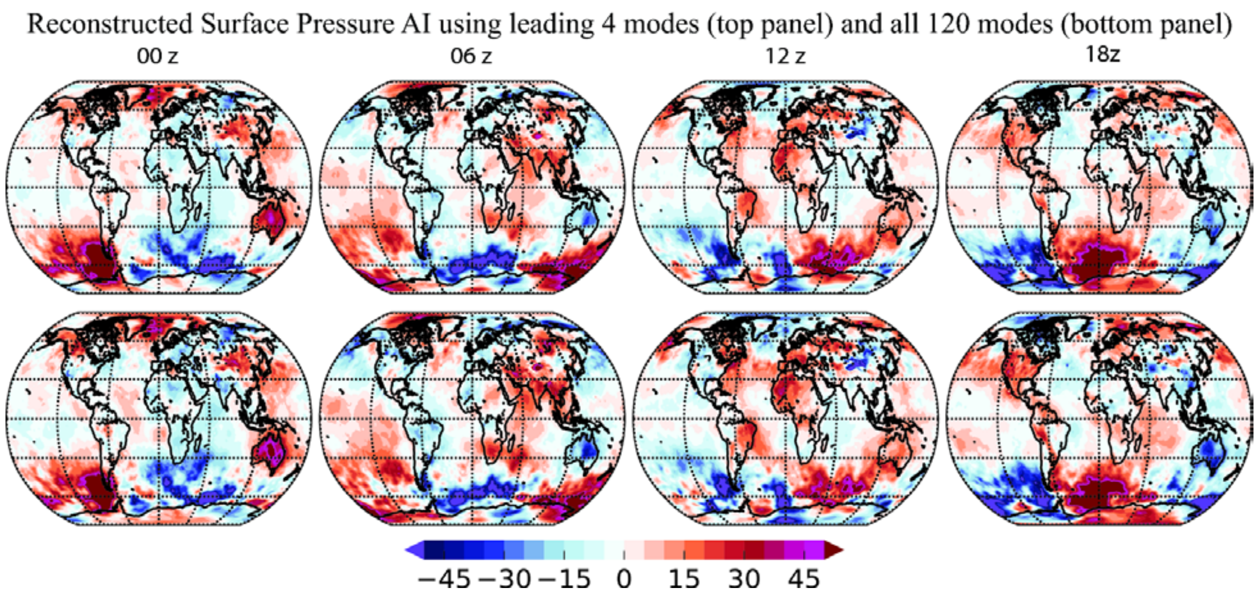

Figure 9. Comparison of the diurnal cycle (September, 2014) constructed using the first four modes for (top row) with the total diurnal cycle (bottom row) errors at 00Z, 06Z, 12Z and 18 Z (left to right) for surface pressure. This is also true for other variables in different months (not shown).

5 Summary and Discussion

In this paper, we estimate the model deficiencies in the Global Forecasting System (GFS) that lead to systematic errors in the forecast, as a first step towards correcting them online (i.e., within the model) as in *Danforth and Kalnay* 2008. For this, we examine six-hour averaged AIs for the years 2012-2016. AIs are the difference between the gridded analysis and forecast, with the former providing our best gridded estimate of the true state of the atmosphere. They contain information about the physical processes that the model lacks and give the best estimate of the systematic errors arising due to model deficiencies. The 6-hr cycle time is sufficiently short that the errors are still linear. This reduces the likelihood of having errors in one variable at one location inducing errors in another variable at a different location, and thus simplifies the identification of causes of the errors.

Our results reveal the presence of significant bias that is geographically anchored with continental scales in the GFS. The model has excess heating and drying of south and east Asia especially during JJA, which leads to a lower pressure forecasts. A likely cause is weaker moisture-carrying monsoon winds from the Southern Hemisphere, which also affects monsoon convection and circulation. Warm and dry anomalies are also present in the regions where GFS is unable to maintain sufficient stratus clouds, i.e. the zone west of South Africa, and the Americas.

At higher latitudes, the oceans have a cold bias during local summer with northward displacement of the band of intense easterlies over the Southern Ocean. The amplitude of the bias declines in 2015, especially over the ocean. We are able to identify one possible cause of the reduction in the Northern Hemisphere, which was the switch in 2015 to an improved, higher spatial and temporal resolution in the estimation of SST boundary conditions. However, the bias represented by AIs over oceans in 2012-2014 are not completely due to model deficiencies, but also arise from bias in prescribed SSTs and a problem with observational assimilation. The mean bias is also reduced over the Southern Ocean in 2015. In this region, the change in SST has less impact. Instead, we think the reduction in bias is due to updating of the Community Radiative Transfer Model and improvements in radiance assimilation.

In addition to time mean bias, we find strong daily bias in temperature, surface pressure, specific humidity, and winds. Specific humidity has a strong diurnal bias pattern while the periodic component of temperature bias shows a complex pattern, with both semidiurnal and diurnal components, where polarity changes every 6-hrs at some places and every 12 hours at other places. The daily biases are similar from 2012 to 2014, and are almost perfectly captured by the four leading EOFs, computed every month, for surface pressure, temperature, and humidity for all months. The amplitude of the daily biases also declines in 2015, especially over the ocean. Here also, we think the decline in bias is due to the improved SST boundary conditions.

Our results for bias estimation in GFS support the application of the approaches used by *DKM*07 to correct the mean and diurnal systematic errors. As the error growth in the short-term is still linear, we can use the estimated model bias corrections and add them as a forcing term in the model tendency equation. With the best estimate of model biases prior to non-linear growth, the challenge that now arises is how to utilize the past estimates to correct present models. An important challenge in using the past AIs as correction for model bias is accounting for contributions of observation biases to the AIs. If the observations have negligible errors, for short-term, the AIs represent the bias due to lack of model dynamics. But AIs should be adjusted for observation biases before using them to correct the model bias. The presence of observation bias can be tested by their impact on the online correction of the bias, since erroneously correcting the model for an observation bias should result in an increase of the AIs.

In the continuation of this work, we plan to use the successful approach of *Greybush et al.* [2012], who used the mean of a limited number of past AIs (e.g., the past 15 days) to correct the model online. As diurnal and semidiurnal errors contribute significantly to the total bias, correcting only the mean bias should not be enough. The diurnal and semidiurnal biases dominate the higher frequencies (sub-monthly) in GFS. As these are reproduced by four eigenmodes out of 120 modes, we plan to use the low dimensional approach as used by *Li et al.* [2009] to correct the sub-monthly periodic bias online. Once the corrections for the mean bias and periodic biases are applied, we would test if the forecast bias improvement achieved online is comparable to the standard operational statistical bias correction made *a posteriori*. We also plan to test whether the reducing the mean and periodic bias reduces the forecast random errors during their nonlinear growth.

We emphasize that the ultimate goal of this study is not to empirically correct the model bias and improve the forecasts only. If our results show that this goal can be achieved, this approach can then be used to guide and optimize the design of subgrid-scale physical parameterizations, more accurate discretizations of the model dynamics, boundary conditions, radiative transfer codes, and other potential model improvements that can then replace the empirical correction scheme. The methodology we propose, if successful, can be also used to efficiently check potential improvements by testing whether they reduce the mean Analysis Increments as expected from their design.

Acknowledgments

We gratefully acknowledge the support of the NOAA grant NA16NWS46800009 and of the Indian Monsoon Mission grant MMSERPUnivMarylandUSA-2013 INT5002150. JAC was supported by the National Science Foundation Physical Oceanography Program (OCE1233942). The authors would like to thank Drs. James Jung, Mark Iredell and Henry Juang for their generous guidance on the running of the GFS, and Dr. Glenn White for creating Fig. 1.

Data

The data used was the operational GFS/GDAS data archived and provided by co-author Dr. Fanglin Yang.

References

Buehner, M., J. Morneau, and C. Charette (2013), Four-dimensional ensemble-variational data assimilation for global deterministic weather prediction. Nonlinear Processes Geophys., 20, 669–682.

Chapman, W. and J. Walsh (2007), Simulations of Arctic Temperature and Pressure by Global Coupled Models. J. Climate, 20, 609–632, doi: 10.1175/JCLI4026.1.

Dalcher, A., and Kalnay, E. (1987). Error growth and predictability in operational ECMWF forecasts. Tellus A, 39A(5), 474–491. https://doi.org/10.1111/j.1600-0870.1987.tb00322.x

Danforth, C. M., E. Kalnay, and T. Miyoshi (2007), Estimating and correcting global weather model error, Monthly Weather Review, 135, 281–299.

Danforth, C.M., and E. Kalnay (2008), Using Singular Value Decomposition to Parameterize State-Dependent Model Errors, Journal of the Atmospheric Sciences, 65, 1467-1478.

Danforth, C.M., and E. Kalnay (2008), Impact of online empirical model correction on nonlinear error growth, Geophysical Research Letters, 35, L24805, doi: 10.1029/2008GL036239.

DelSole, T., M. Zhao, P. Dirmeyer, and B. Kirtman (2008), Empirical Correction of a coupled Land-Atmosphere model, Monthly Weather Review, 136, 4063–4076.

DelSole, T., M. Zhao, and P. Dirmeyer (2009), A new method for exploring land-atmosphere dynamics. J. Hydrometeorology, 10, 1040-1050.

Greybush, S. J., R.J. Wilsom, R.N. Hoffman, M.J. Hoffman, T. Miyoshi, K. Ide, T. McConnochie, and E. Kalnay (2012), Ensemble Kalman Filter data assimilation of spectrometer temperature retrievals into a Mars GCM, J. Geophys. Res., 117, E11008, doi:10.1029/2012JE004097.

Hartmann, D.L., T.N. Palmer, and R. Buizza (1996), Finite-Time Instabilities of Lower-Stratospheric Flow. J. Atmos. Sci., 53, 2129–2143.

Johansson, A., and S. Saha, (1989), Simulation of systematic error effects and their reduction in a simple model of the atmosphere, Mon. Weather Rev., 117, 1658 – 1675

Jung, T. (2005), Systematic errors of the atmospheric circulation in the ECMWF forecasting system, Quart. J. Roy. Meteor.Soc, 131, 1045-1073

Jung, T., and A.M. Tompkins (2003), Systematic errors in the ECMWF forecasting system, Technical Memorandum, No. 442, ECMWF, Shinfield Park, Reading RG 29AX, U. K., 72 pp.

Kalnay, E., M. Kanamitsu, R. Kistler, W. Collins, D. Deaven, L. Gandin, M. Iredell, S. Saha, G. White, J. Woollen, Y. Zhu, A. Leetmaa, R. Reynolds, M. Chelliah, W. Ebisuzaki, W. Higgins, J. Janowiak, K.C. Mo, C. Ropelewski, J. Wang, R. Jenne, and D. Joseph (1996), The NCEP/NCAR 40-Year Reanalysis Project. Bull. Amer. Meteor. Soc., 77, 437–471

Kalnay, E., and Z. Toth (1996), The breeding method, Proceedings of the Seminar on Predictability, held at ECMWF on 4–8 September 1995.

Klinker, E., and P. Sardeshmukh (1992), The diagnosis of mechanical dissipation in the atmosphere from large-scale balance requirements, J. Atmos. Sci., 49, 608 – 627

Li, Hong, E. Kalnay, T. Miyoshi and C. M. Danforth (2009), Accounting for model errors in Ensemble Data Assimilation, Monthly Weather Review, 137, 3407-3419.

Lien, G.-Y., T. Miyoshi, and E. Kalnay (2016b), Assimilation of TRMM Multisatellite Precipitation Analysis with a low-resolution NCEP Global Forecast System. Mon. Wea. Rev., 144, 643–661. doi:10.1175/MWR-D-15-0149.1

Murphy, A. H. (1988), Skill scores based on the mean square error and their relationships to the correlation coefficient. Mon. Wea. Rev., 116, 2417–2424.

Reynolds, R.W. and T.M. Smith (1994), Improved Global Sea Surface Temperature Analyses Using Optimum Interpolation. J. Climate, 7, 929–948.

Saha, S. (1992), Response of the NMC MRF model to systematic error correction within integration, Monthly Weather Review, 120, 345–360.

Sela, J. G. (2009), The Implementation of the Sigma Pressure Hybrid Coordinate into the GFS. NCEP, et al. Office Note #461,425 pp.

Thiébaux, J., E. Rogers, W. Wang, and B. Katz (2003), A New High-Resolution Blended Real-Time Global Sea Surface Temperature Analysis. Bull. Amer. Meteor. Soc., 84, 645–656, doi: 10.1175/BAMS-84-5-645.

Vannitsem, S., and Z. Toth (2002), Short-term dynamics of model errors. J. Atmos. Sci., 59, 2594–2604.

Wang, X., D. Parrish, D. Kleist, and J. Whitaker (2013), GSI 3DVar-Based Ensemble–Variational Hybrid Data Assimilation for NCEP Global Forecast System: Single-Resolution Experiments. Mon. Wea. Rev., 141, 4098–4117.

Wu, W., R.J. Purser, and D.F. Parrish (2002), Three-Dimensional Variational Analysis with Spatially Inhomogeneous Covariances. Mon. Wea. Rev., 130, 2905–2916.

Xue, H.-L., X.-S. Shen, and J.-F. Chou (2013), A forecast error correction method in numerical weather prediction by using the recent multiple-time evolution data. Adv. Atmos. Sci., 30(5), 1249–1259, doi: 10.1007/s00376-013-2274-1.

Xue, H. L., X. S. Shen, and J. F. Chou (2015), An online model correction method based on an inverse problem Part I—Model error estimation by iteration. Adv. Atmos. Sci., 32(10), 1329–1340, doi: 10.1007/s00376-015-4261-1.

Zheng, F., J. Zhu, R.-H. Zhang, and G.-Q. Zhou (2006), Ensemble hindcasts of SST anomalies in the tropical Pacific using an intermediate coupled model. Geophys. Res. Lett., 33, L19604, doi: 10.1029/2006GL026994.

Zheng, F., J. Zhu, H. Wang, and R.-H. Zhang (2009), Ensemble hindcasts of ENSO events over the past 120 years using a large number of ensembles. Adv. Atmos. Sci., 26(2), 359–372, doi: 10.1007/s00376-009-0359-7.

Zheng, Y., T. Shinoda, J. Lin, and G. Kiladis (2011), Sea Surface Temperature Biases under the Stratus Cloud Deck in the Southeast Pacific Ocean in 19 IPCC AR4 Coupled General Circulation Models. J. Climate, 24, 4139–4164, doi: 10.1175/2011JCLI4172.1.